Dynamics of nonlinear blue photoluminescence and Auger recombination in SrTiO3

AUTHOR(S):

Yasuda, Hideki; Kanemitsu, Yoshihiko

PHYSICAL REVIEW B **77**, 193202 (2008)

Dynamics of nonlinear blue photoluminescence and Auger recombination in $SrTiO_3$

Hideki Yasuda[1] and Yoshihiko Kanemitsu[1,2,*]
[1]*Institute for Chemical Research, Kyoto University, Uji, Kyoto 611-0011, Japan*
[2]*Photonics and Electronics Science and Engineering Center, Kyoto University, Kyoto 615-8510, Japan*
(Received 25 January 2008; revised manuscript received 12 March 2008; published 29 May 2008)

We report that the blue photoluminescence (PL) dynamics are dependent on both the photogenerated and the chemically doped carrier densities in $SrTiO_3$. We found that the PL decay dynamics are well explained using a simple model that includes nonradiative single-carrier trapping, radiative bimolecular recombination, and nonradiative Auger recombination processes. In highly photoexcited $SrTiO_3$ and heavily electron-doped $SrTiO_3$, the rapid Auger recombination of the polarons determines the PL properties.

DOI: 10.1103/PhysRevB.77.193202 PACS number(s): 78.55.−m, 73.50.Gr, 78.47.Cd

Transition metal oxides and their heterostructures have attracted a great deal of attention as new device materials due to their wide variety of fascinating and multifunctional properties.[1,2] With its unique electrical and optical properties, $SrTiO_3$ is one of the most important oxide materials both from a fundamental physics viewpoint and from its potential for device applications. The electron density and, hence, the conductivity of $SrTiO_3$ can be controlled by chemical substitution or annealing in a reducing atmosphere.[3,4] It has also been reported that the electron-doped $SrTiO_3$ becomes a superconductor at low temperatures.[5,6] Furthermore, a high-density, two-dimensional electron gas with unique electrical and thermoelectric properties forms at interfaces between $SrTiO_3$ and other oxides.[7,8] Despite extensive studies of the electronic structures and electrical properties of $SrTiO_3$ and related materials,[3–13] the carrier dynamics that determine these electronic and optical properties remain unclear even in the $SrTiO_3$ bulk samples. This is because $SrTiO_3$ shows a strong electron–phonon interaction and shows the formation of polarons and/or self-trapped excitons,[14,15] and has impurities and defects.[16,17] Recently, we reported that electron-doped $SrTiO_3$ samples show blue photoluminescence (PL) at room temperature.[18] As PL spectroscopy is one of the most powerful methods for studying carrier recombination processes in semiconductors, room-temperature PL provides a new opportunity for understanding $SrTiO_3$ carrier dynamics and recombination.

In this Brief Report, we studied the blue PL dynamics of nondoped $SrTiO_3$ under a wide range of excitation densities at room temperature. PL dynamics are sensitive to the photogenerated carrier density. We found that the PL decay dynamics can be well explained by the radiative bimolecular recombination, nonradiative single-carrier trapping, and nonradiative Auger recombination processes. In La- and Nb-doped $SrTiO_3$ samples, the PL lifetime is determined by the doped electron density. In low electron-density samples, the PL intensity and decay properties are determined by the nonradiative single-carrier trapping. In highly photoexcited $SrTiO_3$ and heavily electron-doped $SrTiO_3$, the rapid Auger recombination of polarons determines the PL intensity and dynamics.

Nondoped $SrTiO_3$, $Sr_{1-x}La_xTiO_3$, and $SrTi_{1-y}Nb_yO_3$ crystals [0.5 mm thick with a (100) surface], grown by the Verneuil method (Furuuchi Chemical Co.), were used in this study. To reduce the oxygen vacancies, they were annealed under oxygen flow for 24 h at 700 K. Annealed samples were primarily used; however, there were no significant differences in the PL properties between the as-prepared and the annealed samples. Time-resolved PL spectra were measured at room temperature using a streak camera with a time resolution of 40 ps and a monochromator. The excitation light source was an optical parametric amplifier system based on a regenerative amplified mode-locked Ti:sapphire laser. The excitation wavelength was 355 nm (3.49 eV) with a pulse duration of 150 fs and a repetition rate of 1 kHz. The laser spot size on the sample surface was carefully measured using the knife-edge method.

The inset of Fig. 1 shows a typical time-integrated PL spectrum of nondoped $SrTiO_3$ under 0.02 mJ/cm^2 laser irradiation with the broad PL band observed at around 2.9 eV. This spectral shape is consistent with the PL spectra of electron-doped $SrTiO_3$ samples.[18] The broken curve shows the absorption spectrum; the abrupt increase in optical density corresponds to the Urbach tail below the band gap en-

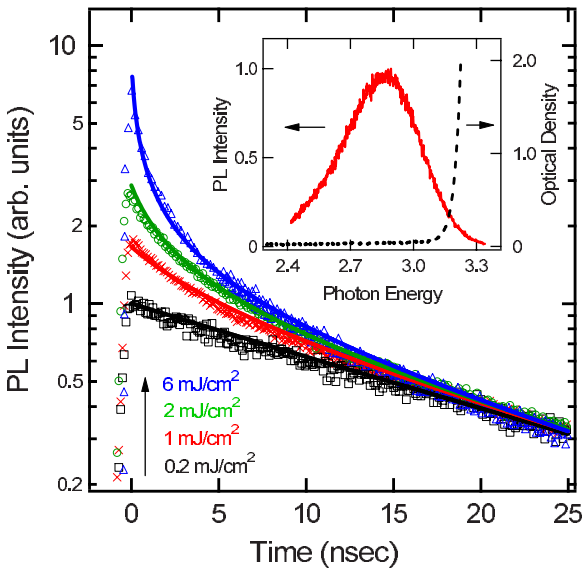

FIG. 1. (Color online) Excitation density dependence of the PL dynamics in nondoped $SrTiO_3$. Fits to the data using Eq. (1) are shown as solid lines. The inset shows the PL spectrum of nondoped $SrTiO_3$ under 0.02 mJ/cm^2 laser irradiation as the solid line and the absorption spectrum as the broken line.

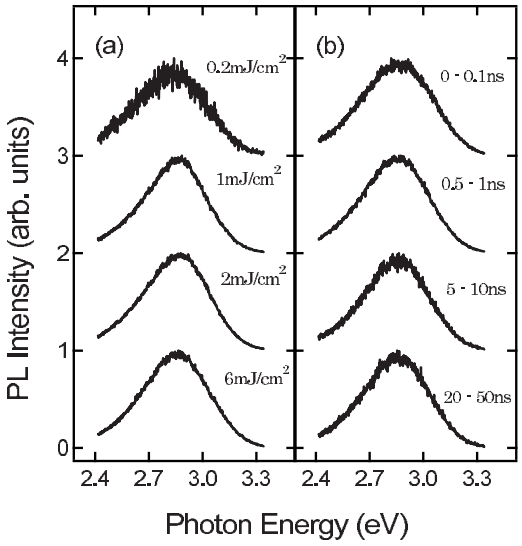

FIG. 2. (a) Excitation density dependence of the time-integrated PL spectra in nondoped $SrTiO_3$. (b) The time-resolved PL spectra of $SrTiO_3$ at different delay times under 6 mJ/cm^2 laser irradiation. The spectra are normalized to their maxima.

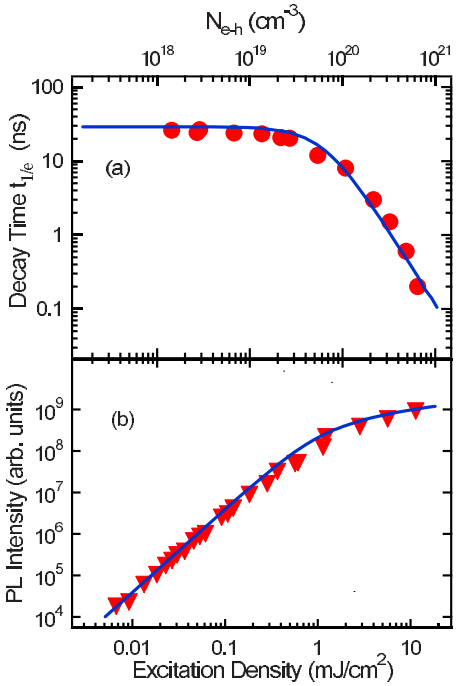

FIG. 3. (Color online) (a) Excitation density dependence of the PL decay time in nondoped $SrTiO_3$. (b) The integrated PL intensity as a function of the excitation density. The solid lines show the calculation result using the obtained parameter A and C, and Eq. (1).

ergy at 3.27 eV.[19] The difference between the band gap energy and the emission peak energy (Stokes shift) is 0.3–0.4 eV. This suggests that the blue PL is not due to the free electrons in the conduction band and the free holes in the valence band but shows the formation of polaron states due to the strong electron–phonon coupling in $SrTiO_3$.[14,20]

Figure 1 shows the PL decay curves around 2.9 eV for nondoped $SrTiO_3$ at different excitation densities. The PL decay dynamics are very sensitive to the excitation density. Under weak excitation (<0.5 mJ/cm^2), the PL decay curve is well described by a single-exponential function. When the excitation density exceeds about 1 mJ/cm^2, a nonexponential component clearly appears in the early stage. With an increase in the excitation intensity, the fast and nonexponential decay component increases.

Figure 2(a) shows the time-integrated PL spectra of nondoped $SrTiO_3$ for different excitation intensities, where the PL spectral shapes were obtained by integrating between 0 and 50 ns. These time-integrated spectral shapes are independent of the excitation intensity. Figure 2(b) shows the PL spectra at different delay times under 6 mJ/cm^2 laser irradiation. The PL spectral shapes are also independent of the delay time although the nonexponential decay component is clearly seen in the early stages. Under high excitation, the spectral shape of the nonexponential component is consistent with that of the single-exponential component under weak excitation. These observations show that the PL spectrum and dynamics are determined by a simple recombination process.

The excitation intensity dependencies of the time-integrated PL intensity and the PL decay time in nondoped $SrTiO_3$ are summarized in Fig. 3. Here, the effective decay time $t_{1/e}$ is defined as the time at the intensity of I_0/e, where I_0 is the PL intensity at zero delay time. The photogenerated electron-hole pair density (N_{e-h}) is estimated from the incident photon number and the optical absorption coefficient at the excitation energy.[21] Under weak excitation density below about 0.5 mJ/cm^2, the PL decay time is constant (about 30 ns) but the PL intensity increases quadratically with the excitation density. At high intensities, the shortening of the PL lifetime and the saturation of the PL intensity occur simultaneously. This behavior can be explained in terms of a nonradiative Auger recombination process, as discussed below.

The high dielectric constant ($\varepsilon \sim 300$) of $SrTiO_3$ reduces the excitonic effects so that nongeminate recombination processes are dominant at room temperature.[14] At high excitation densities, the numbers of electrons and holes are considered to be equal. The rate equation for the photocarriers can therefore be simplified and written as follows:[22]

$$\frac{dn}{dt} = -An - Bn^2 - Cn^3, \tag{1}$$

where n is the photocarrier density. An represents the nonradiative single-carrier trapping and Bn^2 represents the radiative bimolecular recombination. Finally, C is the coefficient of the nonradiative Auger recombination including three-particle, electron-hole-electron, and electron-hole-hole processes, where the nonradiative recombination energy of the electron-hole pairs is transferred to the kinetic energy of the other electron (hole). As the quantum efficiency at room temperature is very low (<0.01), we cannot determine the value of the coefficient B experimentally: The temporal changes in the carrier density are determined by the nonradiative processes of single-carrier trapping and Auger recombination. First, we calculated A to be 1.7×10^7 s^{-1} by fitting the de-

cays under the weak excitations because the single-exponential component is independent of the excitation density. Next, the Auger coefficient was obtained through a one-parameter (C) numerical fit procedure. The excellent fits are shown as solid curves in Fig. 1 where the resultant Auger coefficient is $(1.3 \pm 0.4) \times 10^{-32}$ cm^6/s. In addition, the experimental results in Fig. 3 also reproduced well by the calculation result using the obtained parameter A and C, and Eq. (1). This coefficient is much lower than that of a typical semiconductor such as Si or GaAs.[23,24] Taking into account the large band gap energy and large effective mass of $SrTiO_3$, this value seems reasonable.[22] The nonradiative Auger recombination process is accompanied by a reduction in the PL lifetime and the saturation of the PL intensity. These characteristic features are clearly observed in our experiments with $SrTiO_3$.

It was reported that at low temperatures, the formation of self-trapped excitons through the polarons contributes to the broad PL in the green spectral region.[14,25] The detailed PL mechanism has not been determined because of the unclear role of defects and impurities.[17] There have been several reports of the nonlinear behavior of the blue PL in nondoped $SrTiO_3$ samples, which noted that its origin is complicated.[17,26,27] However, with highly photoexcited $SrTiO_3$ samples, the intrinsic polaron-related PL is observed clearly in the present study. Similar nonlinear PL dynamics are observed at different temperatures (8–300 K). In addition, the carrier-density dependence of the decay time is also observed in the electron-doped samples under weak excitation conditions, as discussed later. Therefore, the heating-related processes do not play a primary role in our PL experiments. As mentioned above, the PL dynamics in $SrTiO_3$ can be well explained using a simple rate equation that includes radiative bimolecular and nonradiative Auger recombination processes.

To further clarify the importance of the Auger recombination process, we examined the PL decay dynamics in $Sr_{1-x}La_xTiO_3$ (La-STO) and $SrTi_{1-y}Nb_yO_3$ (Nb-STO), as semiconductor Auger coefficients are usually determined from measured carrier lifetimes in heavily doped samples.[22,23] The electron densities of these doped samples were estimated from the values reported previously,[6,27,28] assuming a linear relationship between the carrier density and the dopant concentration. In $Sr_{1-x}La_xTiO_3$, the electron density N_e is approximately given by $N_e = 1.80 \times 10^{22} \times x$ cm^{-3}, and in $SrTi_{1-y}Nb_yO_3$ as $N_e = 1.78 \times 10^{22} \times y$ cm^{-3}. In our doped samples, the electron density is higher than the Mott transition density.[4] However, because of the large effective mass and the large dielectric constant of $SrTiO_3$, the plasma frequency is relatively low.[29] Then, the blue PL is clearly observed in heavily doped samples. Using these samples, we measured the PL dynamics as a function of dopant concentration. In these weak excitation experiments, the photogenerated carrier density (N_{e-h}) was about 3×10^{17} cm^{-3}, which was much lower than N_e. The PL decay curves in La-doped $SrTiO_3$ samples are plotted in Fig. 4. All decay curves are approximately described by single-exponential functions (solid curves in the figure). The rate of PL decay becomes faster with an increase in the dopant concentration or the chemically doped electron density.

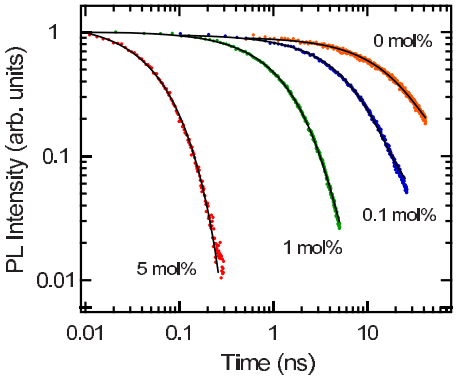

FIG. 4. (Color online) Log–log plot of the PL dynamics of La-doped $SrTiO_3$. The excitation density was about 5 μJ/cm^2. The solid curves show the results of exponential fitting. The data are normalized to their maxima.

In Fig. 5, the PL decay time and PL intensity in the doped samples are summarized as a function of dopant concentration and doped electron density. In heavily electron-doped samples, the PL decay time τ_{PL} is determined by both the single-carrier trapping and the electron-hole-electron Auger recombination,[22]

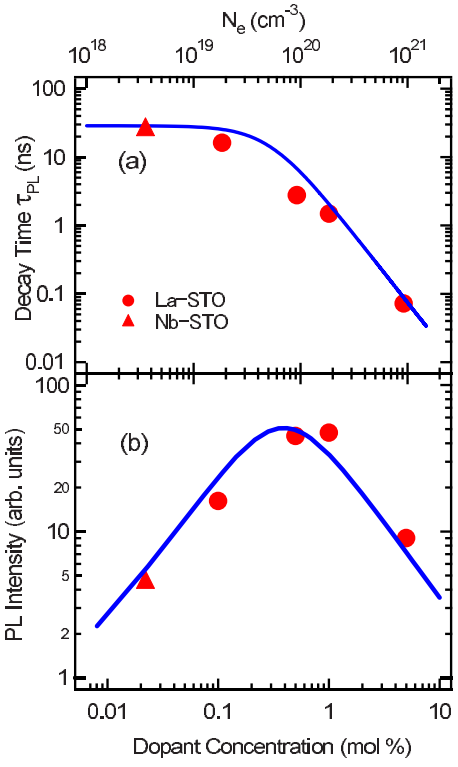

FIG. 5. (Color online) (a) PL decay time and (b) PL intensity of the electron-doped $SrTiO_3$ as a function of the dopant concentration. The solid lines show the numerical calculation results using Eqs. (2) and (3). The upper axis of the electron density was estimated from Refs. 6, 27, and 28, assuming a linear relationship between the dopant concentration and carrier density.

$$\tau_{\mathrm{PL}}^{-1} = 2A + C_1 N_e^2, \tag{2}$$

where C_1 is the coefficient of the electron-hole-electron Auger recombination. The PL intensity is given by the product of N_e and the number of holes $p(t)$,

$$I \propto \int BN_e p(t)dt, \tag{3}$$

The numerical calculations using Eqs. (2) and (3) are plotted as solid curves. The constants A and C were obtained from the nondoped $SrTiO_3$ measurement in Fig. 3, i.e., $A=1.7\times10^7 s^{-1}$, $C=1.3\times10^{-32}$ cm^6/s, and we assumed $C_1 \sim C$ because nondoped $SrTiO_3$ is an n-type semiconductor. Our model can explain quantitatively the enhancement of the PL intensity observed in electron-doped $SrTiO_3$. In the low electron-density region, the PL intensity increases with the doped electron density N_e, according to Eq. (3). In the high electron-density region, on the other hand, the nonradiative Auger recombination determines the PL properties. These calculations agree quite well with the experimental observations in the doped samples. It is considered that the single-carrier nonradiative decay rate increases with the doped electron density. However, the bimolecular radiative and the nonradiative Auger rates are sensitive to the electron density, compared with that of the single-carrier trapping. Therefore, the nonradiative Auger recombination process determines the PL dynamics.

With highly excited $SrTiO_3$ and intentionally electron-doped $SrTiO_3$ samples, the intrinsic PL dynamics can be well explained by a simple model including the nonradiative single-carrier trapping, the radiative bimolecular recombination, and the nonradiative Auger recombination processes influenced by the strong electron–phonon coupling. The first determination of the Auger recombination coefficient provides a new method for the study of the carrier density and its spatial profile in bulk $SrTiO_3$ and $SrTiO_3$-based heterostructures.

In conclusion, we examined the PL dynamics of nondoped $SrTiO_3$ and electron-doped $SrTiO_3$ as a function of photo- and chemical-doped carrier densities. In undoped $SrTiO_3$, a fast-decay and nonexponential PL component was observed in the nanosecond time region under high excitation. In electron-doped $SrTiO_3$, the PL lifetime decreases with an increase of the doped electron density under weak excitation. These experimental data were well explained by a simple model including the nonradiative single-carrier trapping, the radiative bimolecular recombination, and the nonradiative Auger recombination processes. Our finding shows the importance of the multiparticle recombination processes in $SrTiO_3$.

The authors would like to thank T. Tayagaki and Y. Yamada of Kyoto University for helpful discussions. This study was supported in part by a Grant-in-Aid for Scientific Research from the Japan Society for the Promotion of Science.

*Corresponding author; kanemitu@scl.kyoto-u.ac.jp

[1] M. Imada, A. Fujimori, and Y. Tokura, Rev. Mod. Phys. **70**, 1039 (1998).
[2] W. Eerenstein, N. D. Mathur, and J. F. Scott, Nature (London) **442**, 759 (2006).
[3] H. P. R. Frederikse, W. R. Thurber, and W. R. Hosler, Phys. Rev. **134**, A442 (1964).
[4] O. N. Tufte and P. W. Chapman, Phys. Rev. **155**, 796 (1967).
[5] J. F. Schooley, W. R. Hosler, and M. L. Cohen, Phys. Rev. Lett. **12**, 474 (1964).
[6] H. Suzuki, H. Bando, Y. Ootuka, I. H. Inoue, T. Yamamoto, K. Takahashi, and Y. Nishihara, J. Phys. Soc. Jpn. **65**, 1529 (1996).
[7] A. Ohtomo and H. Y. Hwang, Nature (London) **427**, 423 (2004).
[8] H. Ohta, S. Kim, Y. Mune, T. Mizoguchi, K. Nomura, S. Ohta, T. Nomura, Y. Nakanishi, Y. Ikuhara, M. Hirano, H. Hosono, and K. Koumoto, Nat. Mater. **6**, 129 (2007).
[9] A. Fujimori, I. Hase, M. Nakamura, H. Namatame, Y. Fujishima, Y. Tokura, M. Abbate, F. M. F. de Groot, M. T. Czyzyk, J. C. Fuggle, O. Strebel, F. Lopez, M. Domke, and G. Kaindl, Phys. Rev. B **46**, 9841 (1992).
[10] F. Gervais, J. L. Servoin, A. Baratoff, J. G. Bednorz, and G. Binnig, Phys. Rev. B **47**, 8187 (1993).
[11] N. Nakagawa, H. Y. Hwang, and D. A. Muller, Nat. Mater. **5**, 204 (2006).
[12] A. Kalabukhov, R. Gunnarsson, J. Börjesson, E. Olsson, T. Claeson, and D. Winkler, Phys. Rev. B **75**, 121404(R) (2007).
[13] G. Herranz, M. Basletić, M. Bibes, C. Carrétéro, E. Tafra, E. Jacquet, K. Bouzehouane, C. Deranolt, A. Hamzić, J. M. Broto, A. Barthélémy, and A. Fert, Phys. Rev. Lett. **98**, 216803 (2007).
[14] T. Hasegawa, M. Shirai, and K. Tanaka, J. Lumin. **87-89**, 1217 (2000).
[15] H. Okamura, M. Matsubara, K. Tanaka, K. Fukui, M. Terakami, H. Nakagawa, Y. Ikemoto, T. Moriwaki, H. Kimura, and T. Nanba, J. Phys. Soc. Jpn. **75**, 023703 (2006).
[16] K. Szot, W. Speier, R. Carius, U. Zastrow, and W. Beyer, Phys. Rev. Lett. **88**, 075508 (2002).
[17] S. Mochizuki, F. Fujishiro, and S. Minami, J. Phys.: Condens. Matter **17**, 923 (2005).
[18] D. Kan, T. Terashima, R. Kanda, A. Masuno, K. Tanaka, S. Chu, H. Kan, A. Ishizumi, Y. Kanemitsu, Y. Shimakawa, and M. Takano, Nat. Mater. **4**, 816 (2005).
[19] M. Capizzi and A. Frova, Phys. Rev. Lett. **25**, 1298 (1970).
[20] A. S. Barker, Jr., Phys. Rev. **145**, 391 (1966).
[21] M. Cardona, Phys. Rev. **140**, A651 (1965).
[22] P. T. Landsberg, *Recombination in Semiconductors* (Cambridge University Press, Cambridge, 1991).
[23] J. Dziewior and W. Schmid, Appl. Phys. Lett. **31**, 346 (1977).
[24] U. Strauss, W. W. Rühle, and K. Köhler, Appl. Phys. Lett. **62**, 55 (1993).
[25] L. Grabner, Phys. Rev. **177**, 1315 (1969).
[26] A. Rubano, D. Paparo, F. Miletto, U. Scotti di Uccio, and L. Marrucci, Phys. Rev. B **76**, 125115 (2007).
[27] T. Okuda, K. Nakanishi, S. Miyasaka, and Y. Tokura, Phys. Rev. B **63**, 113104 (2001).
[28] S. Ohta, T. Nomura, H. Ohta, and K. Koumoto, J. Appl. Phys. **97**, 034106 (2005).
[29] H. Y. Hwang, Nat. Mater. **4**, 803 (2005).